

Water clarity characteristics during rainfall season revealing impacts of recent deforestation on the fjord-like basin of inner Ambon Bay in the small island of Ambon, eastern Indonesia

^{1,2}Richard R. Lokollo, ^{1,3}Alex S. W. Retraubun, ^{1,3}Simon Tubalawony, ^{1,3}Harold J. D. Waas, ^{4,5}Sem Likumahua, ^{4,5}Gerry G. Salamena

¹Marine Sciences Study Program, Postgraduate Program of Pattimura University, Ambon – Indonesia; ²Department of Physics, Faculty of Sciences and Technology, Pattimura University, Ambon – Indonesia; ³Faculty of Fisheries and Marine Sciences, Pattimura University, Ambon – Indonesia; ⁴Research Center for Deep-Sea of National Research and Innovation Agency (BRIN), Jakarta – Indonesia; ⁵Centre for Collaborative Research on Aquatic Ecosystem in Eastern Indonesia (Pusat Kolaboratif Riset Ekosistem Perairan Indonesia Timur), Ambon, Indonesia. Corresponding author: R. R. Lokollo, richard.lokollo@lecturer.unpatti.ac.id

Abstract. A water clarity study was conducted during the wet season in inner Ambon Bay (IAB), a fjord-like basin isolated from outer Ambon Bay (OAB; the offshore open ocean) by a narrow-shallow sill. This geomorphology is rare in Indonesia, and it has been exposed to increased freshet linked to recent rapid deforestation. The main goals of this study were (i) to reveal how the IAB isolation determines the turbid classification of the basin (categories ranging from low-turbid condition to ultra-high-turbid condition according to scientific literature), based on the light attenuation coefficient (K_d) and turbidity, and (ii) to assess how significant light attenuation affects light limitation for primary producers in the basin such as phytoplankton and seagrass based on the ratio of euphotic depth (Z_{eu}) and surface mixed layer depth (Z_m). This study also predicted total suspended solids (TSS) using K_d . Oceanographic measurements (vertical turbidity profiling, Secchi depth, surface light intensity) in IAB were undertaken during the wet season and subsequently indicated that IAB was surprisingly classified as a moderate-turbid environment (based on K_d and TSS values) instead of supposedly a high-turbid condition concerning the prevailing wet season with frequent freshet coupled with the IAB isolation. Moreover, light attenuation in IAB during the wet season played a minimal role in limiting light for primary producers due to the prevailing $Z_{eu}:Z_m > 1$. The potential cause for the moderate-turbid status coupled with high light availability in the isolated IAB was likely linked to rapid flushing in IAB that can quickly flush suspended sediments out of the basin, hence preventing the establishment of high turbidity.

Key Words: light attenuation, turbidity, light limitation, water clarity, inner Ambon Bay.

Introduction. In the aquatic environment, water clarity is a key aspect of water quality since water clarity is commonly used to indicate the level of suspended sediment, a ubiquitous water pollutant that is widely known for harmful effects on the environment particularly on aquatic organisms (Clark et al 1985; Effler 1988; Davies-Colley & Smith 2001). The impacts of suspended sediment on aquatic organisms through the effects of suspended sediment on water clarity are mainly via the light attenuation process by which the intensity of light penetrating the water column reduces due to suspended sediment distributed within the water column (Henley et al 2000). The adverse effects of light attenuation on aquatic organisms are mainly twofold. Firstly, light attenuation by suspended sediment significantly affects the light availability for aquatic primary producers (e.g. phytoplankton; seagrass) with low water clarity due to significant light attenuation resulting in light limitation for primary producers (Kirk

1994; Kelble et al 2005). The sediment-induced light attenuation also negatively affects the trophic interactions in the aquatic system due to the reduced water clarity (Vogel & Beauchamp 1999; Nurminen & Horppila 2006; Lunt & Smee 2014; Reustle & Smee 2020). Besides the ecological-related impacts, the reduced water clarity by suspended sediment greatly affects the public's perception of whether the aquatic environment is considered for recreation activities (Effler 1988; Angradi et al 2018). Due to water clarity as a proxy to gauge suspended sediment pollution, water clarity monitoring has been conducted in many countries to continuously assess the water quality status of their water bodies, e.g., in Australia regarding dredging and coastal mining (Mulhearn 1993) in the US such as in the Gulf of Mexico estuaries receiving massive river runoff from the mainland (Smith et al 2006) and in Chesapeake Bay (Turner et al 2021); in lakes (Bai et al 2020) and coastal oceans (Lu et al 2024) in China; and Europe such as in Baltic Sea (Kahru et al 2022) and English Channel (Vantrepotte et al 2012; Capuzzo et al 2015).

Practically, the degree of light attenuation, represented by the light attenuation coefficient (K_d ; unit: m^{-1}), can be used to indicate the level of suspended sediment pollution within the categories of low-to-high turbid conditions, indicating the related low to high level of suspended sediment pollution. For low-turbid condition, the light attenuation coefficient has an interval of $K_d \leq 0.107 \text{ m}^{-1}$ while for moderate-turbid condition, the interval is $0.107 \text{ m}^{-1} < K_d \leq 0.593 \text{ m}^{-1}$ (Shen et al 2010; Shen et al 2013; Sokoletsky & Shen 2013). The aquatic systems classified as high-turbid and ultra-high turbid conditions have the respective ranges of K_d of $0.593 < K_d \leq 4.113 \text{ m}^{-1}$ and $K_d > 4.113 \text{ m}^{-1}$ (Shen et al 2010; Shen et al 2013; Sokoletsky & Shen 2013).

Several factors are driving low water clarity linked to suspended sediment in the aquatic environment. The primary factor is massive river runoff carrying terrestrial-originated sediments into the aquatic systems, e.g., in the northern Gulf of Mexico in the US (Lugo-Fernández et al 2008) and the Great Barrier Reef, Australia (Fabricius 2005; Orpin & Ridd 2012; Fabricius et al 2014). The suspended sediment loads from river runoff coupled with the slow flushing process in isolated basins such as in lakes, fjords, and estuaries can significantly reduce water clarity due to the massive build-up of suspended sediment (Pickard 1961; Carney et al 1999; Lugo-Fernández et al 2008). Besides the river runoff factor, oceanographic processes such as bottom stirring due to tides and winds can also create low water clarity conditions as the stirring process results in bottom sediment resuspension (Larcombe et al 1995; Orpin & Ridd 2012; Whinney et al 2017; Salamena 2024).

The Indonesian archipelago is broadly defined by two continental shelves, with the Sunda Shelf connected to the Asian Continent and the Sahul Shelf linked to the Australian Continent and New Guinea (Figure 1a). These continental shelves are connected to mostly large islands (area $> 100,000 \text{ km}^2$) in the archipelago (except Sulawesi Island), such as Sumatera Island, Kalimantan Island, Java Island, and the Indonesian territory of west New Guinea (Figure 1a). Between these two continental shelves lies deep ocean sub-basins (average depth: 4,000 m) featuring numerous small oceanic islands (area $\leq 2,000 \text{ km}^2$) (Jezek & Hutchison 1978; Pownall et al 2013). The current status of the water quality issues linked to low water clarity in the Indonesian archipelago has been mostly represented by water clarity studies in large islands of the archipelago (with large river catchment areas coupled with a high human population), and the main finding from these studies indicated that coastal waters in these large islands experience significantly low water clarity (Secchi depth: $< 3 \text{ m}$ with an average of 1 m) due to high terrestrial suspended sediment loads; e.g., in Sumatera Island (Amri & Muchlizar 2018; Amri et al 2019; Prasetyo et al 2022; Azwar et al 2023), in Java Island (Helfinalis 2005; Riyadi 2005; Siregar & Koropitan 2013; Dewi et al 2022), in Kalimantan Island (Budhiman 2004; Budhiman et al 2012), in Sulawesi Island (Buana et al 2021; Irawati et al 2023) and Indonesian territory of west New Guinea (Ilahude et al 2004; Alongi et al 2012; Alongi et al 2013). Numerous water clarity studies with more focus on the large Indonesian islands lead to limited knowledge on the topic in the small oceanic islands in the archipelago. This disparity is presumably because massive development in large islands

with large river catchment areas and the resulting high suspended sediment loads discharged into coastal waters commonly attract more attention from researchers than in small oceanic islands (with small river catchment areas and supposedly insignificant suspended sediment loads discharged into coastal waters).

One emerging reason to motivate assessments of water clarity in the coastal waters of small oceanic islands in the Indonesian archipelago is the recent rapid coastal development in the small islands. Due to development resulting from human migration, economic activities, and tourism, coastal urban areas in remote small islands in the archipelago have recently emerged and have been usually accompanied by land clearing activities (e.g. for residential and mining areas); the deforestation has the potential to increase suspended sediment loads into the adjacent coastal waters in the coming years (Pelasula 2008; Male et al 2013; Kakisina et al 2015; Hermawan et al 2017; Akhir 2018). As such, water clarity studies in the small oceanic islands with rapid coastal development in the Indonesian Archipelago are considered to be important for providing insights regarding the status of suspended sediment pollution associated with emerging human activities in the small islands.

Ambon Island (area: $\sim 800 \text{ km}^2$; population: 500,000, source: Indonesian Bureau of Statistics 2010), a small oceanic island in eastern Indonesia (Figure 1b), is considered to be a suitable location to investigate the impacts of rapid coastal development in small islands on potentially the reduced water clarity in the adjacent coastal waters linked to increased suspended sediment inputs. Ambon City in Ambon Island (indicated by the area inside the red line in Figure 1b) serves as the Maluku provincial capital (a rare role played by such a small-sized island in Indonesia) and has rapidly developed in recent decades (following the rapid growth of the human population in the city; Indonesian Bureau of Statistics 1980; Pelasula 2008; Indonesian Bureau of Statistics 2010), more than development rates of other similar-sized islands. The development in Ambon City has resulted in rapid deforestation at the upper lands of Ambon Island has caused increased river runoff in the form of intense freshets, particularly during the wet season (Pelasula 2008; Kakisina et al 2015). As such, Ambon Bay, the adjacent coastal waters, particularly, in the isolated inner Ambon Bay (IAB, Figure 1b and c), is likely to be exposed to suspended sediment pollutants (Pelasula 2008).

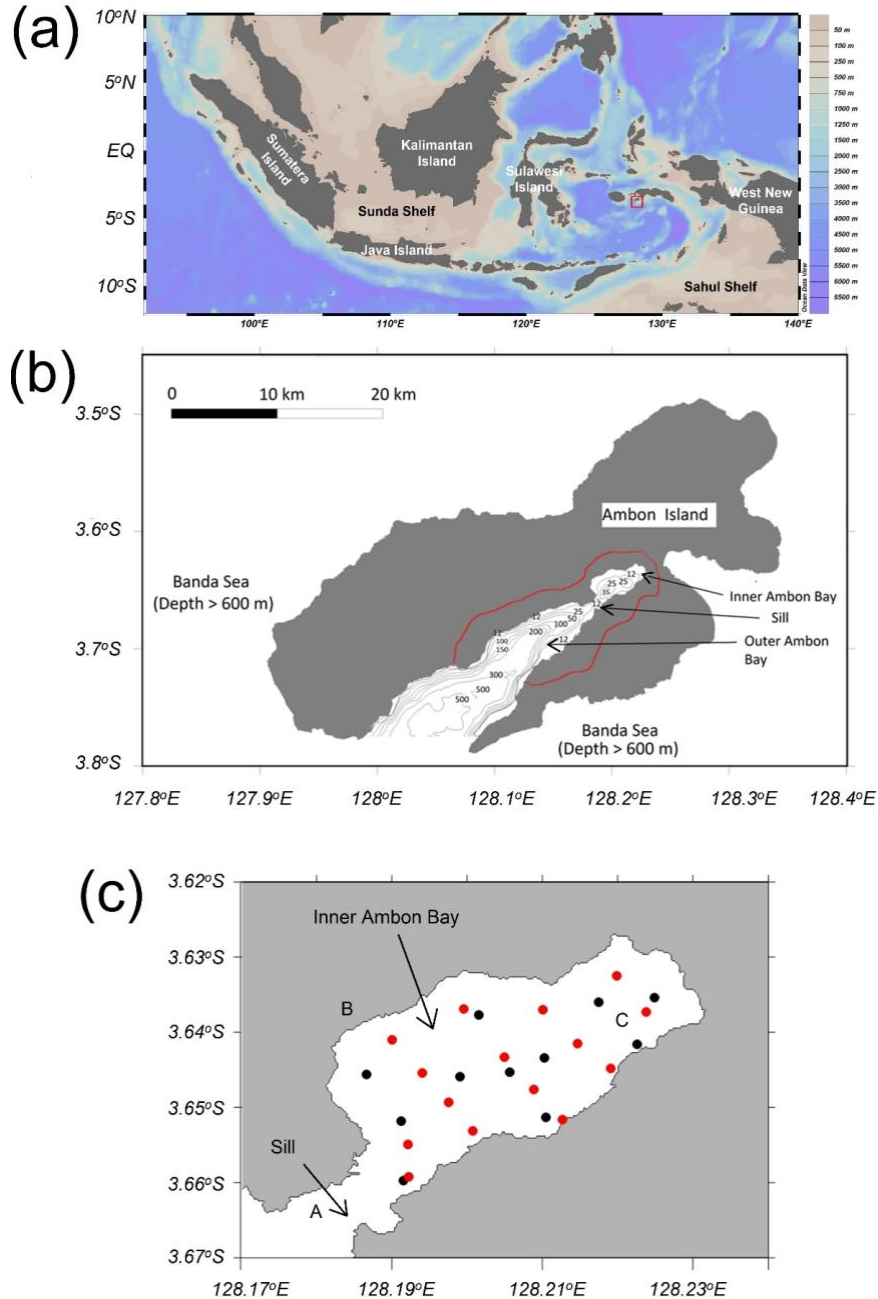


Figure 1. (a) The geography of the Indonesian archipelago with the emphasis on its large islands combined with the associated continental shelves within the archipelago (Sunda and Sahul Shelves); the red box indicates the location of Ambon Island that is zoomed in Figure 1b. (b) The geography of Ambon Island shows the geomorphology and bathymetry (contour) of Ambon Bay consisting of inner Ambon Bay and outer Ambon Bay; the red line indicates the administrative area of Ambon City. (c) The geography of inner Ambon Bay with the emphasis on oceanographic stations (i.e. (•) and (●)) employed in this study. (•) were measured in September 2021 and March 2022 while (●) were measured in August 2023. A (Salamena et al 2021), B (Indonesian Bureau for Spatial Information – BIG), and C (Indonesian Navy-LIPI tidal measurements) represent locations ever used to measure tidal harmonics (currents or water elevation) in IAB.

Despite the suspended sediment threat linked to recently rapid deforestation, the characteristics of water clarity in IAB during the wet season (when intense freshet occurs)

linked to anthropogenic activity are poorly investigated. To date, there are only two existing studies investigating the water clarity characteristics in IAB (Likumahua et al 2019; Wenno 1989). One of these two studies (Wenno 1989) was conducted during the periods when land clearing activities were very low in Ambon Island (in the 1970s-1980s) due to a small human population at that time on the island. Hence, this previous study was not able to reveal the impact of increased suspended sediment input linked to recent rapid deforestation on the water clarity in IAB (Pelasula 2008; Kakisina et al 2015). The other study (Likumahua et al 2019), despite being conducted recently (hence, representing the period of rapid land clearing in Ambon Island), employed very limited observation stations (4 stations) hence inadequately covered the total surface area of IAB (11.5 km²) including sections in the IAB basin nearby the surrounding rivers where freshet is discharged. In addition, this previous study did not particularly discuss water clarity and sediment-caused pollutants that induced light penetration in the IAB basin (Likumahua et al 2019).

There is also a specific interest in investigating water clarity in IAB during the wet season, considering its fjord-like geomorphology. The isolation of a water body from the open water system can result in slow flushing/circulation inside the isolated basin (i.e. commonly found in lakes and fjords) (Crippen & Pavolka, 1970; Syvitski et al 2012), and this possibly leads to the formation of turbid water as terrestrial-originated suspended loads are likely to be trapped inside the isolated basin (hence, reducing water clarity) (Workgroup 2004). Due to the fjord-like geomorphology in IAB where the basin is isolated from its offshore open waters, outer Ambon Bay (OAB), by a narrow-shallow sill (Figure 1b), one would suggest that the IAB isolation might promote low water clarity conditions during the wet season. This is likely due to high suspended loads carried by intense freshet events during the wet season, probably being trapped inside the basin instead of being transported directly to the OAB. Due to the available information on the flushing time of IAB during the wet season (~ 2 weeks) (Pello et al 2014; Salamena et al 2021, 2022b; Salamena et al 2023), the investigation on water clarity in IAB during the wet season could provide important insight on how the flushing capability of IAB (resulting from the IAB isolation) characterizes water clarity inside the basin under high suspended sediment inputs linked to high river runoff during the particular season.

This study sought to reveal the characteristics of water clarity in IAB during the wet season when terrestrial-originated suspended sediments are expected to be considerably discharged into the basin. The water clarity characteristics obtained from this current study aimed to reveal how the continuously rapid land clearing in Ambon Island, coupled with the flushing capability of IAB, affects the water quality of IAB. In this study, the level of water clarity in IAB was represented by the estimates of light attenuation coefficient (K_d) and euphotic depth (Z_{eu}) from Secchi depth and by the measured turbidity. The values of K_d estimated in this current study were used to reveal whether IAB is classified as a low-turbid, moderate-turbid, or high-turbid system. This study also investigated the potential light limitation due to light attenuation by suspended sediment via the ratio of Z_{eu} to the surface mixed layer depth (Z_m). This sought to understand whether the sediment-induced light attenuation in IAB during the wet season can limit light for primary producers, and this is of interest to the water quality management in IAB.

Material and Method

Description of the study sites with an emphasis on inner Ambon Bay. Ambon Bay is a fjord-like basin, formed due to the tectonic collision and bending of two previous islands of volcanic origin (Leitimor and Leihitu) to create the current Ambon Island (Figure 1b) (Jezek & Hutchison 1978; Honthaas et al 1999). Nowadays, the bay is characterized by inner Ambon Bay (IAB; average depth: 25 m; Figure 1b), a shallow semi-enclosed basin that is isolated from outer Ambon Bay (OAB; a steady sloping outer section of Ambon Bay connected to the Banda Sea), by a narrow, shallow sill (12 m) (see Figs. 1b and c) (Salamena et al 2021).

Seasonal conditions and tidal characteristics in IAB. IAB experiences seasonal freshwater inputs. The wet (also called rainfall) season commences in May (the early stage of the wet season), reaches its peak in July to August, and wanes in September – this period is often called easterly monsoonal season due to the prevailing easterly monsoonal winds over Ambon Island (Tarigan 1989; Pello et al 2014). During the wet season, IAB experiences frequent freshet events due to high rainfall over the upper lands of IAB (Pelasula 2008; Saiya et al 2016; Salamena et al 2023). In contrast, the dry season with low freshwater inputs prevails in IAB between December and February (Tarigan 1989). During this season, freshet occurs less frequently in IAB (Pello et al 2014).

IAB is a tidal-dominated basin as supported by a few locations in the basin (i.e. A, B, and C in Figure 1c) showing tidal harmonics. As such, it can be said that the IAB length (longitudinal length from the sill: ~5 km) is also the tidal intrusion length of IAB – this condition might not be applicable for other estuarine-like basins (e.g. river estuaries) when the tidal intrusion length is shorter than the basin's length, causing some sections especially on the farther inland waters that do not experience tidal harmonics (Uncles et al 2002). Tidal cycles in IAB are mixed semidiurnal (Salamena et al 2022a; Salamena et al 2021, 2022b). Spring tides produce a maximum tidal range between flood and ebb of 2.5 m while neap tides only create a 1.2 m tidal range (van Oostenbrugge 2003). The magnitude of the tidal range in IAB is categorized as mesotidal (≥ 2 m and < 4 m) (Uncles et al 2002).

Nutrient inputs and flushing processes in IAB. IAB is a complex system regarding nutrient inputs. The basin receives dissolved nutrients from the land (via river runoff with a maximum supply during the wet season when freshet events occur (Pello et al 2014; Ikhsani et al 2016) and from the open ocean (OAB connected to the Banda Sea) (Ikhsani et al 2016). Yet, the elevated nutrients in IAB commonly occurring during the wet season are not related to the elevated rainfall (Likumahua et al 2019). Instead, it is most likely oceanic nutrients from OAB predominate the nutrient budget in IAB via frequent oceanic inflow replenishing IAB (Salamena et al 2022a; Salamena et al 2021, 2022b). This frequent supply of nutrient-rich oceanic water from OAB regulates the magnitude of flushing in IAB (flushing time: about two weeks).

The main driver for the flushing processes in IAB is tides. Two tidal-induced flushing mechanisms in IAB are deep-water renewal linked to internal tidal waves in OAB (Wenno & Anderson 1984; Salamena et al 2021) and estuarine circulation (i.e. tidal-mean two-layer system) linked to surface brackish water (Salamena et al 2022b). The former mechanism occurs intermittently (i.e. in the form of episodic intruding water pulses) each a spring-neap tidal sequence and replenishes the deep layer of IAB (volume below the sill) (Salamena et al 2021). The latter mechanism occurs regularly following water moving in and out of IAB based on flood/ebb tidal cycles and flushing the surface layer of IAB to the sill depth (~ 12 m) (Salamena et al 2022b).

Theoretical frameworks of light attenuation in the marine environment

Light attenuation coefficient and Secchi depth. According to the Beer-Lambert law, the intensity of light penetrating the water column of the ocean decays exponentially, called light attenuation, and this is mathematically expressed (Macdonald 2015; Weiskerger et al 2018; Glover et al 2019):

$$I(z) = I_0 \exp(-K_d z) \quad (1)$$

where $I(z)$ is the light intensity reaching depth z while I_0 is the initial light intensity before penetrating the ocean (i.e., at $z = 0$). K_d is the light attenuation coefficient – large K_d creates low water clarity (Davies-Colley & Smith 2001).

Practically, K_d is easily determined using a simple tool called Secchi disk, a white-black colored 30-cm disk i.e., the disk is lowered into a certain depth where the white part of the disk is no longer visible and this depth is defined as Secchi depth, Z_{sec} (Erlandsson & Stigebrandt 2006; Bowers et al 2020). At Z_{sec} , the initial light intensity, I_0 , typically reduces to 10% I_0 (Buiteveld

1995; Tyler 1968). Therefore, by applying $I(z) = 10\% I_0$ in Eq. 1 when Z_{sec} is known, the light attenuation coefficient, K_d , is then determined as (Kelble et al 2005):

$$K_d = 2.3/Z_{sec} \quad (2)$$

Euphotic depth and light limitation due to light attenuation in marine systems. Light attenuation in the marine system affects ocean primary producers (e.g. phytoplankton; seagrass) since the attenuation regulates the light availability in the water column to be used for the photosynthesis by the producers (Cloern 1987; Kelble et al 2005). This light availability is commonly represented by the euphotic zone, spanning from the surface depth to a certain depth called euphotic depth, Z_{eu} , where $I(z) = 1\% I_0$ (Kirk 1994; Kelble et al 2005). Hence, using Eq. 1, Z_{eu} is estimated by (Kelble et al 2005):

$$Z_{eu} = 4.61/K_d \quad (3)$$

Light limitation for primary producers due to light attenuation can occur in marine systems when the available light in the water column might not be sufficient for photosynthesis. Light limitation by light attenuation can be adequately assessed using the ratio of euphotic depth (Z_{eu}) to surface mixed layer (Z_m) (Cloern 1987; Kelble et al 2005). When $Z_{eu} \cdot Z_m < 1$, the light attenuation process (i.e. Eq. 1) is considered to have a major role in limiting the growth of ocean primary producers (Kelble et al 2005). In contrast, $Z_{eu} \cdot Z_m > 1$ indicates a minimal role of the light attenuation process in limiting the growth of the primary producers (Kelble et al 2005). In this study, Z_m was determined using the density criterion of 0.05 kg m^{-3} (Brainerd & Gregg 1995).

The decomposition of light attenuation coefficient: contributions of clear seawater and water turbidity components. Light attenuation coefficient, K_d , in seawater represents the degree of seawater clarity that is contributed by the inherent characteristic of seawater itself (e.g. from density regulated by temperature and salinity somehow determining the refractive index of the light) and the turbidity level contained in the seawater (Effler 1988; Macdonald 2015). As such, K_d can be decomposed into two components, light attenuation coefficients due to (i) the clear seawater properties (K_d^{clear}) and (ii) due to turbidity ($K_d^{turbidity}$) (Macdonald 2015) as expressed by:

$$K_d = K_d^{clear} + K_d^{turbidity} = K_d^{clear} + a \times Tu \quad (4)$$

where Tu is the depth-averaged water turbidity (unit: NTU) while a (unit: $\text{m}^{-1} \cdot \text{NTU}^{-1}$) is a coefficient associated with the light attenuation driven by turbidity (Macdonald 2015). The linear relationship in Eq. 4 allows the estimation of K_d^{clear} graphically by plotting scattered data points of the observed Tu versus the estimated K_d with the constant of the linear relationship (i.e. the intercept value) between Tu versus K_d referring to K_d^{clear} (e.g. Figure 40 of Macdonald 2015).

In a turbid environment such as coastal waters and estuaries where the major contribution of turbidity is from suspended sediment, light attenuation coefficient, K_d , in Eq. 4 can be modified to predict the amount of total suspended sediment (TSS; unit: mg L^{-1}) as formulated by Eq. 7 (Bowers et al 2020):

$$K_d = (a^{clear} + a^{turbidity} TSS) / \mu \quad (5)$$

where a^{clear} is the light absorption coefficient of seawater without suspended sediments while μ is the mean cosine of the downwelling light radiation with the value of 0.7 for the turbid

condition (Kirk 1994; Matthes et al 2019). $a^{turbidity}$ is the light absorption coefficient linked to suspended sediments with typical values ranging 0.02-0.06 m² g⁻¹ (Bowers & Binding 2006). From Eq. 4 and Eq. 5, the parameterization of the $K_d^{clear} - a^{clear}$ relationship can be written as:

$$K_d^{clear} = a^{clear} / \mu \quad (6)$$

Thermodynamics-optical balance in predicting K_d^{clear} . The light attenuation coefficient for clear seawater without suspended sediments, K_d^{clear} , can be calculated by combining the warming process of the surface ocean (thermodynamics) with the penetration process of light radiation to the ocean's upper layers (marine optics) and this combination is commonly known as the water radiant heating rate theory (Ohlmann & Siegel 2000; Wei & Lee 2013). Imagine that the surface ocean with the initial near-surface water temperature of T_0 is warmed by the sun. After a warming duration of dt , the near-surface water temperature elevates to be T_1 . Hence, the degree of warming is equivalent to dT/dt . Meanwhile, optically, the surface ocean also experiences light attenuation during the warming process when light radiation from the sun penetrates the water column (see Eq. 1). The water radiant heating rate theory indicates that this warming process can be balanced mathematically with this optical process, subsequently, indicating that the light attenuation process is primarily regulated by the elevated water temperature (Wei & Lee 2013). As such, the light attenuation process here is more likely to be driven by the change of density due to the warming process; hence, only K_d^{clear} is relevant here. This thermodynamics-optical balance is mathematically expressed as (Ohlmann & Siegel 2000; Wei & Lee 2013):

$$\rho C_p \frac{dT_{near-surface}}{dt} = - \frac{dI(z)^{clear}}{dz} \quad (7)$$

where ρ is the near-surface water density subject to the warming process, C_p is the specific heat capacity of seawater ($\sim 4,700$ J kg⁻¹ °C⁻¹) and $dT_{near-surface} / dt$ is the rate of temperature change at the near-surface layer due to the warming. $I(z)^{clear} = I_o \exp(-K_d^{clear} z)$ is the exponential decay of light radiation due to the inherent characteristics of clear seawater without suspended sediments. Applying the derivation of z to $I(z)^{clear}$, Eq. 7 becomes:

$$\frac{\rho C_p}{I_o} \frac{dT_{near-surface}}{dt} = K_d^{clear} \exp(-K_d^{clear} \cdot z) \quad (8)$$

Applying the natural logarithm to both sides, Eq. 8 is now written as:

$$\ln\left(\frac{\rho C_p}{I_o} \frac{dT_{near-surface}}{dt}\right) = \ln K_d^{clear} - K_d^{clear} \cdot z \quad (9)$$

In Eq. 9, I_o , $dT_{near-surface} / dt$ and ρ can be easily obtained from field measurements with $dT_{near-surface} / dt$ that can be obtained by measuring surface water temperature in a location during early warming in the morning to the peak of the warming around the noon. z can also be determined as a certain surface depth experiencing the warming process. This hence leaves the unknown K_d^{clear} to be determined. To estimate K_d^{clear} , Eq. 9 needs to be reformulated to be:

$$F(K_d^{clear}, z) = \ln K_d^{clear} - K_d^{clear} \cdot z - \ln\left(\frac{\rho C_p}{I_o} \frac{dT_{near-surface}}{dt}\right) = 0 \quad (10)$$

where $F(K_d^{clear}, z)$ is a function that is equal to zero. Here, a certain value of K_d^{clear} causing $F(K_d^{clear}, z) = 0$ is then considered to be the light attenuation coefficient of clear seawater obtained from the thermodynamic-optical balance.

Classification of turbid environment based on the magnitude of light attenuation coefficient and TSS. The water clarity in the marine system can be classified based on the magnitude of the light attenuation coefficient (K_d) (Shen et al 2010; Shen et al 2013; Sokoletsky & Shen 2013), as shown in Table 1. Low-turbid condition is represented by $K_d \leq 0.107 \text{ m}^{-1}$ while moderate-turbid condition is classified by $0.107 \text{ m}^{-1} < K_d \leq 0.593 \text{ m}^{-1}$ (Shen et al 2010; Shen et al 2013; Sokoletsky & Shen 2013). In addition, the high-turbid condition is indicated by $0.593 \text{ m}^{-1} < K_d \leq 4.113 \text{ m}^{-1}$ while the ultra-high turbid condition is met when $K_d > 4.113 \text{ m}^{-1}$ (Shen et al 2010; Shen et al 2013; Sokoletsky & Shen 2013).

Table 1
Classification of turbid conditions in marine environments based on K_d and TSS

<i>The classification of turbid condition in marine system</i>			
	$K_d \text{ (m}^{-1}\text{)}$		$TSS \text{ (mg L}^{-1}\text{)}$
Low-turbid condition	$K_d \leq 0.107$	Low-turbid condition	$TSS < 5$
Moderate-turbid condition	$0.107 < K_d \leq 0.593$	Moderate-turbid condition	$5 < TSS < 50$
High-turbid condition	$0.593 < K_d \leq 4.113$	High-turbid condition	$TSS > 50$
Ultra-high turbid condition	$K_d > 4.113$		

Similar to the water clarity classification based on K_d , the turbid condition in the marine system can also be categorized using TSS concentration (Table 1). Low turbid condition is classified by TSS concentration less than 5 mg L^{-1} , while moderate turbid condition has a TSS interval of $5 < TSS < 50 \text{ mg L}^{-1}$. High turbid condition is categorized by $TSS > 50 \text{ mg L}^{-1}$.

Oceanographic measurements. This study employed oceanographic stations inside IAB covering a large portion of the surface area of the IAB basin (Figure 1c). In general, the measurements at the stations were conducted in three stages of wet seasons: the early stage of the wet season in May 2022, the peak of the wet season in August 2023, and the waning of the wet season in September 2021 (Table 2). The focus of this study on the wet season in IAB was linked to the high probability of the basin being exposed to significant run-off discharge (compared to the other seasons with low rainfall), likely affecting water clarity in the embayment. In all stages of the wet season, at the oceanographic stations (Figure 1c), vertical profiles of turbidity and the light intensity above the surface ocean were measured (Table 2). Vertical profiles of temperature, salinity, and density from a Conductivity-Temperature-Depth (CTD) instrument (type: SWIFT Valeport CTD) were measured during the peak and waning stages of wet seasons while Secchi depth was measured only during the peak of the wet season (Table 2). Regarding the timing for sampling in the chosen stages of the wet season in relationship to the optimum solar insolation, the measurements were conducted between 10:00 hours and 14:00 hours when irradiance angles are expected to be close to the solar zenith (Macdonald 2015).

The procedures for calculating K_d and Z_{eu} are based on the data availability in IAB in the wet season. This section aims to describe sequentially the calculation process of K_d and Z_{eu} in this study regarding the data availability in three sampling periods described in Table 2. Firstly, the calculations of the light attenuation coefficient (K_d ; Eq. 2) and the subsequent

euphotic depth (Z_{eu} ; Eq. 3) were undertaken using the August 2023 datasets that included Secchi depth measurements (Table 2). Due to the absence of Secchi depth measurements in the sampling periods of September 2021 and May 2022 (Table 2), K_d in these periods was determined using the linear relationship between K_d and turbidity, which was measured in these sampling periods (Table 2). To do this, the parametrization of the K_d -turbidity linear relationship ($K_d = K_d^{clear} + a \times Tu$; Eq. 4) was first established from the August 2023 datasets measuring both Secchi depth and turbidity. Then, K_d for the sampling periods of September 2021 and May 2022 were estimated by inputting the measured turbidity data from these periods (Table 2) into the obtained linear formula. As K_d in the sampling periods of September 2021 and May 2022 was calculated, the associated Z_{eu} values were subsequently computed (Eq. 3).

Table 2

Metadata of oceanographic measurements in IAB in this study

<i>Sampling period</i>	<i>Station locations in IAB</i>	<i>Parameters measured in the oceanographic stations</i>
September 2021 (the waning of wet season)	Indicated by (•) in Figure 1c	Vertical profiles of temperature, salinity, density and turbidity Light intensity just above the surface ocean
May 2022 (the early stage of wet season)		Vertical profiles of turbidity Light intensity just above the surface ocean
August 2023 (the peak of wet season)	Indicated by (•) in Figure 1c	Vertical profiles of temperature, salinity, density and turbidity Light intensity just above the surface ocean Secchi depth

Results

Light attenuation and turbidity in IAB in the wet season. In general, the light attenuation coefficient, K_d , and the resulting euphotic depth (Z_{eu}) in IAB changed following the strength of the wet season. During the early stage of the wet season in May 2022 when rainfall was not intensified, the mean values of K_d and Z_{eu} in IAB were found to be 0.42 m^{-1} and 10.48 m, respectively. As the wet season reached its peak in August 2023 (hence, the maximum rainfall rate), the mean values of K_d (0.56 m^{-1}) and Z_{eu} (8.23 m) were found to be respectively higher and shallower than that of the early stage of wet season. As the wet season waned in September 2021, K_d (0.48 m^{-1}) and Z_{eu} (9.6 m), respectively, slightly decreased and deepened in comparison to those found during the peak of the wet season.

The pattern of the mean values of the depth-averaged turbidity in IAB (measured using turbidity profiler) was generally consistent with K_d (measured using Secchi disk), concerning the stages of wet season (the early stage of wet season: 0.72 NTU; the peak of wet season: 1.00 NTU; the following waning stage of wet season: 0.88 NTU).

From the light attenuation-turbidity relationship in IAB during the wet season ($K_d = 0.37$ [depth-averaged turbidity] + 0.15; $R^2 = 0.46$; Figure 2), an empirical formula to estimate turbidity by simply using Secchi depth, Z_{sec} , was obtained. Using Eq. 2 substituted into the light attenuation-turbidity relationship, the parametrization of the turbidity- Z_{sec} relationship

for IAB during the wet season was found to be: [depth-averaged turbidity] = [1 / (0.37 Z_{sec})] (2.3 – 0.15 Z_{sec}).

Light attenuation by clear seawater in IAB in the wet season: the estimation of K_d^{clear} and a_{clear} . In general, the light attenuation coefficient of clear seawater, K_d^{clear} , in IAB was found to be $0.15 \pm 0.03 \text{ m}^{-1}$. For instance, from the August 2023 datasets, the linear relationship between the depth-averaged turbidity and the light attenuation coefficient (K_d ; as shown in Figure 2) resulted in $K_d^{clear} = 0.15 \text{ m}^{-1}$, obtained as the constant of the linear regression relationship (Eq. 4; see also label in Figure 2). This was applied due to the absence of zero turbidity measured in IAB which acted as the intercept in the linear regression formula. Additionally, using the thermodynamics-optical balance (§3.1.4), K_d^{clear} was found to be $0.13 \pm 0.01 \text{ m}^{-1}$ and $0.17 \pm 0.01 \text{ m}^{-1}$ for the August and September sampling periods, respectively; note, K_d^{clear} was not able to be estimated in the May sampling period due to the absence of CTD profiles (see Table 2).

Moreover, the absorption coefficient of clear seawater (a_{clear}) in IAB during wet season (using Eq. 6) was found to be $0.105 \pm 0.014 \text{ m}^{-1}$ utilizing the K_d^{clear} values from the turbidity- K_d relationship (Eq. 5; 0.15 m^{-1}) and the thermodynamics-optical balance (§3.1.4; 0.13 and 0.17 m^{-1}).

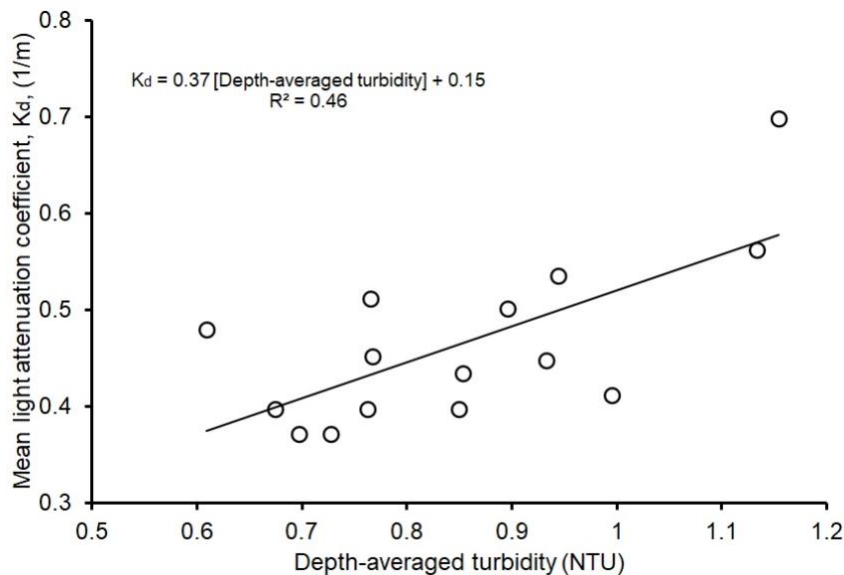


Figure 2. The linear relationship between depth-averaged turbidity and Secchi-derived light attenuation coefficient in IAB during the August 2023 sampling period.

TSS concentration is derived from light attenuation. The mean values of TSS concentration in IAB estimated using Eq. 5 varied following the strength of the wet season (Table 3). The TSS concentration was calculated to be 2.6 mg L^{-1} during the early stage of the wet season. The predicted TSS elevated to 7.2 mg L^{-1} during the peak of the wet season and decreased during the waning of the wet season (5.7 mg L^{-1}).

Table 3

Mean values of predicted TSS during the stages of wet season in IAB

Sampling period	Mean TSS concentration (mg L^{-1})
-----------------	---

May (early stage of wet season)	2.6
August (the peak of wet season)	7.2
September (waning stage of wet season)	5.7

Light limitation for ocean primary producers linked to light attenuation in IAB. Based on $Z_{eu}:Z_m$ (see §3.1.2), light attenuation in IAB during the wet season was found to play a minimal role in limiting light for ocean primary producers in the system. Z_m (using the density criterion of 0.05 kg m^{-3}) in IAB during the wet season was found to be ranging 1.5-2.5 m, significantly shallower than Z_{eu} (i.e. 8.23 – 10.48). Hence, $Z_{eu}:Z_m$ was found to be larger than 1 and this did not meet the condition in which light attenuation has a major impact in limiting light for ocean primary producers (i.e. $Z_{eu}:Z_m < 1$).

Classification of turbid condition in IAB in the wet season. In general, IAB during the wet season was found to be categorized as a moderate-turbid environment. This was based on the mean values of K_d (i.e., the early stage of wet season: 0.44 m^{-1} ; the peak of wet season: 0.56 m^{-1} ; the waning of wet season: 0.48 m^{-1}) and TSS concentration (the early stage of wet season: 2.6 mg L^{-1} ; the peak of wet season: 7.2 mg L^{-1} ; the waning of wet season: 5.7 mg L^{-1}) (Table 3) that met the moderate-turbid condition presented in Table 1.

Discussion

Turbidity controls water clarity in IAB in the wet season. Turbidity controls the variability of light attenuation in IAB during the wet season. The variation in the degree of depth-averaged turbidity measured during the stages of the wet season such as the early stage (0.72 NTU), the peak (1.00 NTU) and the waning (0.88 NTU) resulted in the associated variability in light attenuation coefficients (the early stage of wet season: 0.44 m^{-1} ; the peak of wet season: 0.56 m^{-1} ; the following waning stage of wet season: 0.48 m^{-1}).

The linear relationship between turbidity and light attenuation in this current study agrees with previous studies in other coastal basins. This includes coastal inner shelf waters of the Great Barrier Reef in North Queensland, Australia using the observed turbidity (NTU) versus light attenuation coefficient (MacDonald), and some coastal waters in the North America region that used the measured TSS (mg L^{-1}) versus light attenuation coefficient e.g. in San Francisco Bay (Cloern 1987), New York Bight (Malone 1976) and in Delaware Bay (Pennock 1985).

Prevailing moderate-turbid conditions in IAB in the wet season

Compared with previous studies. This current study agrees with the recent water clarity study in IAB (Likumahua et al 2019) regarding the prevailing moderate-turbid condition in IAB during the wet season. For instance, the values of K_d estimated from this study ($0.44\text{-}0.56 \text{ m}^{-1}$) and the previous study ($0.2\text{-}0.35 \text{ m}^{-1}$; their Figure 4c) meet the moderate-turbid condition category ($0.107 < K_d \leq 0.593$; Table 1). It is interesting to note that K_d calculated in this study was found to be 1.6 to 2 times higher than that of Likumahua et al (2019). The difference is likely linked to the use of more stations in this current study (Figure 1c) that covered more sections near coasts in IAB where relatively lower water clarity exists compared to very few stations employed by Likumahua et al (2019) (Figure 1).

Hydrodynamics drivers regulating the moderate-turbid condition in IAB in the wet season. The status of moderate-turbid conditions in IAB during the wet season (from the viewpoints of K_d and TSS; §4.5) appears to be regulated by the hydrodynamics of the basin. Uncles et al (2002) investigated the effects of flushing time, tidal intrusion length, and tidal range on turbidity in ~ 50 estuaries and have obtained important insights regarding factors

preventing the occurrence of high turbidity in estuaries. The first insight was that short flushing time in estuaries (0.5 days to up to ~ a few weeks in comparison to long flushing time: > 60 days) allows suspended sediment in the water column (e.g., due to freshets or sediment resuspension) to be rapidly flushed out of the estuaries (e.g., via the ebbing currents of spring tides). The second insight was that the comparable magnitude between the estuarine length and the prevailing tidal excursion in the estuary enables suspended sediment to be flushed out of the system in a single ebb tide. In the context of IAB, the basin has a short flushing time during the wet season driven by frequent oceanic intrusions from OAB (i.e., within 2 weeks; Salamena et al 2021, 2022b) despite its low tidal range (mastoidal; Uncles et al 2002; van Oostenbrugge 2003). In addition, the basin has a tidal intrusion length of 5 km (see §2.2) that is comparable with the prevailing maximum tidal excursion during spring tides in the system (i.e. 5-7 km; Salamena et al 2021; their Figs. 5e and f) – this can allow terrestrial-originating suspended sediments in IAB due to freshet to be flushed out of the system within a single ebb during spring tides. As such, the IAB basin during the wet season meets the requirements for conditions that prevent the establishment of high turbidity in estuaries reported by Uncles et al (2002), consistent with the observations in this current study showing the prevailing moderate-turbid status in IAB during the wet season (see § 4.5).

The light attenuation coefficient in IAB reveals the water exchange process between IAB and OAB. In this current study, the estimates of light attenuation coefficient (K_d) in IAB, including the clear seawater's light attenuation coefficient (K_d^{clear}) seem to unveil the exchange process between IAB and OAB. Despite the general isolation of IAB from OAB due to a narrow-shallow sill located between these basins (Figure 1), IAB has been reported to be regularly flushed within spring-neap tidal sequences by oceanic water from OAB (Wenno & Anderson 1984; Salamena et al 2022a; Salamena et al 2021, 2022b). The intruding water from OAB reaching IAB is likely to be mixed with the IAB resident water, and this can modify the inherent characteristics of the intruding water, such as salinity, temperature (Salamena et al 2022a), or also turbidity content. Regarding the turbidity content, the modification process can be revealed from the spatial evolution in the magnitude of K_d from OAB to IAB. Likumahua et al (2019) measured K_d in OAB and IAB during the wet season with respective values of 0.15 m^{-1} and $0.2\text{-}0.35 \text{ m}^{-1}$ (their Figure 4c). Meanwhile, from this current study, K_d and K_d^{clear} in IAB during the wet season were calculated to be $0.42\text{-}0.56 \text{ m}^{-1}$ and $0.15\pm 0.03 \text{ m}^{-1}$, respectively. Considering (i) $K_d = K_d^{clear} + K_d^{turbidity}$ (turbidity component; see Eq. 4) (Bowers et al 2020; Macdonald 2015) and (ii) the high-frequent flushing in IAB by the OAB intruding water, the very similar values between K_d in OAB (0.15 m^{-1}) and K_d^{clear} in IAB ($0.15\pm 0.03 \text{ m}^{-1}$) indicate that low-turbid water from OAB (indicated by smaller K_d) reaching IAB has been modified within IAB via the increase of the turbidity content, indicated by the elevation of K_d (Likumahua et al 2019; also this current study).

Insignificant light limitation for primary producers in IAB in the wet season

Potential causes. The insignificant role of light attenuation in limiting light for ocean primary producers in IAB in the wet season (i.e. $Z_{eu}: Z_m > 1$; §4.4) is likely to be caused simultaneously by the deepening of Z_{eu} and the shallowing of Z_m . Regarding the deepening of Z_{eu} (8.23 – 10.48 m), the condition is likely to be related to the moderate-turbid status in IAB during the wet season (§4.5), linked to the hydrodynamics aspects in the embayment that likely prevent the establishment of high turbidity (e.g. rapid flushing and tidal characteristics; see §5.2.2). Regarding the shallowing of Z_m (1.5-2.5 m; §4.4) in IAB during the wet season, the condition is likely to be driven by the establishment of surface density stratification (Cloern, 1987) due to surface brackish water in the wet season (the top 5 m) (Pello et al 2014; Salamena et al 2022b) that suppresses surface mixed layer depth.

The impacts on the existing knowledge of primary productivity in IAB. This current study adds an important insight into the existing knowledge supporting IAB as a productive

marine ecosystem. Cloern (1987) indicated that productive marine ecosystems can be justified by (i) the availability of high nutrient concentration and (ii) adequate light availability represented by the insignificant light limitation that both favorably support the growth of primary producers. Regarding IAB, the former aspect has been recently unveiled in the form of the tidal-induced frequent supply of oceanic water with high nutrients originating from OAB into IAB (Salamena et al 2022a; Salamena et al 2021, 2022b). The latter aspect, for the first time, is presented through this current study that demonstrates a minimal light limitation condition in IAB, resulting in sufficient light availability for primary producers.

The combination of high nutrient supply from OAB into IAB and minimal light limitation in IAB during the wet season may explain why IAB experiences elevated levels of primary productivity during this time. Reports of high primary productivity levels in IAB have predominantly occurred during the wet season (Likumahua 2013; Sidabutar et al. 2000; Salamena et al. 2022a; Sidabutar et al. 2022). Regarding nutrient enrichment driving high primary productivity, Salamena et al. (2022a) recently demonstrated that high primary productivity levels, attributed to Chl-a concentrations exceeding 5 mg m^{-3} , likely happen in IAB during the wet season when a sufficient volume of dense intruding water from OAB raises IAB's deep resident water from depths of 26-30 m to around 5-6 m. However, the previous study did not investigate the water clarity aspect that supports the high primary productivity observed at the 5-6 m depth in IAB (see Figure 4a and b). This limitation was addressed in the current study. For example, this research showed that the surface depths with high primary productivity, as reported by Salamena et al. (2022a), were located within the euphotic zone (within the top 8.23 – 10.48 m). This condition allows phytoplankton communities at the 5-6 m depth in IAB to thrive under high nutrient conditions (Salamena et al. 2022a) and abundant light availability (as demonstrated in this study), thus promoting the establishment of substantial phytoplankton biomass.

Along with the aspect of water clarity in IAB during the wet season that supports high primary productivity, the predicted TSS in IAB during the wet season (as noted in this study) appears to satisfy a general condition for establishing high phytoplankton biomass. Earlier studies (Wofsy 1983; Cloern 1987) have pointed out that high phytoplankton biomass can only occur when TSS concentrations are below 50 mg L^{-1} . Beyond this threshold ($>50 \text{ mg L}^{-1}$), marine environments are categorized as high-turbidity environments (Table 1), where phytoplankton communities face severe light limitation (Wofsy 1983; Cloern 1987). For IAB, the TSS concentration in the basin during the wet season was measured to be less than 10 mg L^{-1} (Table 3), which supports the likelihood of high primary productivity occurring in the basin.

Lessons learned from the water clarity characteristics in IAB in the wet season

A simple algorithm to predict TSS in IAB in the wet season. This current study provides a low-cost, robust approach for water quality monitoring and management in IAB via the use of a Secchi disk for predicting water turbidity. Water clarity is widely considered to be a key indicator to assessing the level of water quality in an aquatic environment (Effler 1988), and the Secchi disc, a low-cost device, has continuously been considered to be an effective tool for providing a quick and simple estimate of water clarity (Tyler 1968; Preisendorfer 1986; Bowers et al 2020; Golubkov & Golubkov 2024). The parameterization of the Secchi depth (Z_{sec})-turbidity relationship (i.e. [depth-averaged turbidity] = $[1/(0.37 Z_{sec})]$ ($2.3 - 0.15 Z_{sec}$); §4.1) for IAB during wet season presented here allows water quality managers and local environmental authorities in IAB to easily obtain a quick, rough estimate of turbidity in IAB during the particular season by simply measuring Secchi depth.

Prevailing rapid flushing in IAB overshadowing the impacts of recently rapid deforestation in Ambon Island in controlling water clarity in IAB. Moderate-turbid condition in IAB during the wet season (presented here) indicates that rapid flushing in IAB mitigates the impact of intense freshet containing highly suspended sediment linked to

recently rapid land clearing activities. The development in Ambon City has led to rapid deforestation in the upper lands of Ambon Island (Pelasula 2008; Syahailatua et al 2012; Kakisina et al 2015). This has caused increased river runoff in the form of intense freshets that carry high suspended sediment, particularly during the wet season, into IAB (Pelasula 2008). Once entering the IAB water body, the suspended solids are subject to the flushing capacity of the basin. The early water clarity study in IAB in the wet season, Wenno (1989), conducted during the period when land clearing activities were very low in Ambon Island (in the 1970s-1980s), indicated that considerably low water clarity during a significant freshet event in IAB can be significantly improved in the following 6 hours, coincidentally with the prevailing semi-diurnal tidal cycle in the basin. The previous study, hence, argued that this rapid change in water transparency might be linked to tidal-induced rapid flushing in IAB (Wenno 1989). At the time (in the 1970s-1980s), the knowledge of IAB flushing was very limited to support this rapid flushing argument; recent oceanographic studies ultimately have confirmed this rapid flushing argument (Salamena et al 2021, 2022b). Meanwhile, the assessment of water clarity in IAB during the wet season under the scenario of recent rapid deforestation in Ambon Island in this current study surprisingly does not contradict Wenno (1989). This current study demonstrates that IAB still maintains its generally moderate-turbid condition (§4.5). The persistent moderate-turbid condition in IAB throughout time, such as between the period of 1970s-1980s with insignificant deforestation as reported by Wenno (1989) and recent years with intense deforestation (i.e. in 2021-2023) means that the rapid flushing in IAB plays a key role in preventing the establishment of high turbidity in the basin despite the recent elevated suspended sediment inputs in the basin.

Conclusions. The water clarity characteristics in IAB during the wet season (May- September) were represented by the mean values of the light attenuation coefficient (K_d), the euphotic depth (Z_{eu}), and depth-averaged turbidity ranging from 0.42-0.56 m^{-1} , 8.23-10.48 m and 0.72-1.00 NTU, respectively. The predicted TSS concentration derived from K_d in IAB during the wet season was found to be 2.7-7.2 $mg L^{-1}$. Based on the estimated values of K_d and TSS, IAB was found to be categorized as a moderate-turbid condition during the wet season. In addition, the light attenuation coefficient for clear seawater was found to be $0.15 \pm 0.03 m^{-1}$, while the associated absorption coefficient of clear seawater was $0.105 \pm 0.014 m^{-1}$.

Light limitation for primary producers due to the light attenuation process was found to be minimal in IAB during the wet season due to the ratio of Z_{eu} (8.23-10.48 m) to the surface mixed layer depth (1.5-2.5 m) larger than 1. The moderate-turbid status in IAB during the wet season is thought to be linked to rapid flushing in the basin that can remove suspended sediments in the water column of IAB instantly, hence preventing the establishment of high turbidity in the basin. This might characterize the marine chemistry, such as the nutrient properties in the basin. Previous studies such as Balls (1994) and Loder & Reichard (1981) have reported that flushing time has the potential to control the characteristics of dissolved nutrients in estuaries, i.e., rapid flushing in estuaries results in the nutrients likely behaving conservatively. This is likely to apply to IAB with rapid flushing and moderate turbid status, although this topic is beyond the scope of the current study. Future studies on the nutrient dynamics linked to the flushing and the suspended sediments of IAB would be required to fill this scientific gap.

It should be noted that the moderate-turbid status in IAB during the wet season revealed in this current study does not preclude the potential impacts of recent deforestation in Ambon Island on IAB from the viewpoint of the transport of coarse-sized sediment pollutants. This current study confines its focus on the characteristics of water clarity in the water column of IAB during the wet season, which is primarily affected by fine-sized sediment, easily carried by ocean flow and surface brackish water. The tendency of fine-sized sediment to be more easily transported by ocean flow and brackish water than coarse-sized sediment results in the distribution of coarse-sized sediment being generally concentrated near river mouths of IAB (Pelasula 2008). The investigation of the distribution and transport

characteristics of coarse-sized sediment pollutants near river mouths in IAB, including the quantification of sedimentation rate, can provide important insights regarding the impacts of recent deforestation in Ambon Island on IAB.

In addition, due to the characteristics of water clarity presented here, their impacts on the population of phytoplankton in IAB from ecological viewpoints are likely to be significant. Future studies that collect phytoplankton samples during the wet season are likely to reveal how the water clarity characteristics in this particular season can affect the phytoplankton diversity and assembly.

Acknowledgements. We would like to thank the CTD operator and the boat skipper for their field assistance during the oceanographic measurements.

Conflict of interest. The authors declare no conflict of interest.

References

- Akhir K., 2018 A critical analysis of technological interventions towards the national action plan for marine litter management 2018-2025: recommendations for addressing marine plastic litter in the 'new Bali' of Indonesia sustainably.
- Alongi D. M., da Silva M., Wasson R. J., Wirasantosa S., 2013 Sediment discharge and export of fluvial carbon and nutrients into the Arafura and Timor Seas: A regional synthesis. *Marine Geology* 343:146-158.
- Alongi D. M., Wirasantosa S., Wagey T., Trott L. A., 2012 Early diagenetic processes in relation to river discharge and coastal upwelling in the Aru Sea, Indonesia. *Marine Chemistry* 140:10-23.
- Amri K., Ma'mun A., Priatna A., Suman A., Prianto E., Muchlizar, 2019 [Abundance and spatial-temporal distributions of phytoplankton in Siak River estuary in relation to oceanographic parameters]. *Majalah Ilmiah Globè* 21(2):105-116. [in Indonesian]
- Amri K., Muchlizar M., 2018 [Characteristics of physical oceanography in Bengkalis estuary based on in-situ measurements]. *Jurnal Segara* 14(1):43-56. [in Indonesian]
- Angradi T. R., Ringold P. L., Hall K., 2018 Water clarity measures as indicators of recreational benefits provided by US lakes: Swimming and aesthetics. *Ecological Indicators* 93:1005-1019.
- Azwar E., Sularno S., Waruwu F. P., Tarigan M. R. I. M. A., Ulfa S. W., Djaingsastro A. J., 2023 Diversity of penaeidae at the Mengkudu Bay Waters, North Sumatra, Indonesia. *Biodiversitas Journal of Biological Diversity* 24(3):1376-1384.
- Bai S., Gao J., Sun D., Tian M., 2020 Monitoring water transparency in shallow and eutrophic lake waters based on GOCI observations. *Remote Sensing* 12(1):163.
- Balls P. W., 1994 Nutrient inputs to estuaries from nine Scottish east coast rivers; influence of estuarine processes on inputs to the North Sea. *Estuarine, Coastal and Shelf Science* 39(4):329-352.
- Bowers D. G., Roberts E. M., Hogue A. M., Fall K. A., Massey G. M., Friedrichs C. T., 2020 Secchi disk measurements in turbid water. *Journal of Geophysical Research: Oceans* 125(5):e2020JC016172.
- Bowers D., Binding C., 2006 The optical properties of mineral suspended particles: A review and synthesis. *Estuarine, Coastal and Shelf Science* 67(1-2):219-230.
- Brainerd K. E., Gregg M. C., 1995 Surface mixed and mixing layer depths. *Deep Sea Research Part I: Oceanographic Research Papers* 42(9): 1521-1543.
- Buana S., Tambaru R., Selamat M. B., Lanuru M., Massinai A., 2021 The role of salinity and Total Suspended Solids (TSS) to abundance and structure of phytoplankton communities in estuary Saddang Pinrang. In *IOP Conference Series: Earth and Environmental Science* 869(1):012081.

- Budhiman S., 2004 Mapping TSM concentrations from multisensor satellite images in turbid tropical coastal waters of Mahakam Delta, Indonesia. International Institute for Geoinformation Science and Earth Observation, Enschede, the Netherlands.
- Budhiman S., Salama M. S., Vekerdy Z., Verhoef W., 2012 Deriving optical properties of Mahakam Delta coastal waters, Indonesia using in situ measurements and ocean color model inversion. *ISPRS Journal of Photogrammetry and Remote Sensing* 68:157-169.
- Buiteveld H., 1995 A model for calculation of diffuse light attenuation (PAR) and Secchi depth. *Netherlands Journal of Aquatic Ecology* 29:55-65.
- Capuzzo E., Stephens D., Silva T., Barry J., Forster R. M., 2015 Decrease in water clarity of the southern and central North Sea during the 20th century. *Global change biology* 21(6):2206-2214.
- Carney D., Oliver J. S., Armstrong C., 1999 Sedimentation and composition of wall communities in Alaskan fjords. *Polar Biology* 22:38-49.
- Clark E. H., Haverkamp J. A., Chapman W., 1985 *Eroding Soils. The off-farm impacts.* The Conservation Foundation, Washington. Pp. 13.
- Cloern J. E., 1987 Turbidity as a control on phytoplankton biomass and productivity in estuaries. *Continental shelf research* 7(11-12):1367-1381.
- Crippen J. R., Pavolka B. R., 1970 *The Lake Tahoe Basin, California-Nevada.* US Geological Survey. Pp. 56.
- Davies-Colley R., Smith D., 2001 Turbidity suspended sediment, and water clarity: a review *JAWRA Journal of the American Water Resources Association* 37(5):1085-1101.
- Dewi T. A. R., Mauludiyah M., Munir M., 2022 Study of the relationship of water quality with the ecological index of aquatic biota in The Permata Pilang Beach Estuary Area, Probolinggo. *Jurnal Biota* 8(2):123-131.
- Effler S., 1988 Secchi disc transparency and turbidity. *Journal of Environmental Engineering* 114(6):1436-1447.
- Erlandsson C. P., Stigebrandt A., 2006 Increased utility of the Secchi disk to assess eutrophication in coastal waters with freshwater run-off. *Journal of Marine Systems* 60(1-2):19-29.
- Fabricius K. E., 2005 Effects of terrestrial runoff on the ecology of corals and coral reefs: review and synthesis. *Marine pollution bulletin* 50(2):125-146.
- Fabricius K., Logan M., Weeks S., Brodie J., 2014 The effects of river run-off on water clarity across the central Great Barrier Reef. *Marine pollution bulletin* 84(1-2):191-200.
- Glover H., Ogston A., Miller I., Eidam E., Rubin S., Berry H., 2019 Impacts of suspended sediment on nearshore benthic light availability following dam removal in a small mountainous river: in situ observations and statistical modeling. *Estuaries and Coasts* 42:1804-1820.
- Golubkov M., Golubkov S., 2024 Patterns of the relationship between the Secchi disk depth and the optical characteristics of water in the Neva Estuary (Baltic Sea): the influence of environmental variables. *Frontiers in Marine Science* 11:1265382.
- Helfinalis H., 2005 Distribution of suspended sediment in Jakarta Bay and the Seribu Island waters. *Jurnal Perikanan Universitas Gadjah Mada* 7(2):128-134.
- Henley W., Patterson M., Neves R., Lemly A. D., 2000 Effects of sedimentation and turbidity on lotic food webs: a concise review for natural resource managers. *Reviews in Fisheries Science* 8(2):125-139.
- Hermawan R., Damar A., Hariyadi S., 2017 Daily accumulation and impacts of marine litter on the shores of Selayar Island Coast, South Sulawesi. *Waste Technology* 5(1):15-20.
- Honthaas C., Maury R. C., Priadi B., Bellon H., Cotten J., 1999 The Plio-Quaternary Ambon arc, Eastern Indonesia. *Tectonophysics* 301(3-4):261-281.
- Ikhsani I. Y., Abdul M. S., Lekalet J. D., 2016 [Distribution of phosphate and nitrate in inner Ambon Bay during westerly and easterly monsoons]. *Widyariset* 2(2):86-95. [in Indonesian]

- Ilahude A. G., Hortle K., Kusmanto E., 2004 Oceanography of coastal and riverine waters around Timika, West Central Irian Jaya, Arafura Sea. *Continental shelf research* 24(19):2511-2520.
- Indonesian Bureau of Statistics, 1980 [Projection of population of Maluku Province 1980], Indonesian Bureau of Statistics, Ambon. 126 pp. [in Indonesian]
- Indonesian Bureau of Statistics, 2010 [2010 Census Report: aggregated data per district of Ambon City], Indonesian Bureau of Statistics, Ambon. 15 pp. [in Indonesian]
- Irawati S. L., Muliddin A. A., Gunawan Y., Syamsul R. H., Restele H., 2023 Analysis of water condition based on suspended sediment distribution and phytoplankton abundance in Lasolo Bay, Southeast Sulawesi Province. In *IOP Conference Series: Earth and Environmental Science* 124(1):012029.
- Jezek P., Hutchison C., 1978 Banda arc of eastern Indonesia: petrology and geochemistry of the volcanic rocks. *Bulletin Volcanologique* 41:586-608.
- Kahru M., Bittig H., Elmgren R., Fleming V., Lee Z., Rehder G., 2022 Baltic Sea transparency from ships and satellites: Centennial trends. *Marine Ecology Progress Series* 697:1-13.
- Kakisina T. J., Anggoro S., Hartoko A., Suripin, 2015 Analysis of the impact of land use on the degradation of Coastal Areas at Ambon Bay-mollucas Province Indonesia. *Procedia Environmental Sciences* 23:266-273.
- Kelble C. R., Ortner P. B., Hitchcock G. L., Boyer J. N., 2005 Attenuation of photosynthetically available radiation (PAR) in Florida Bay: Potential for light limitation of primary producers. *Estuaries* 28:560-571.
- Kirk J. T., 1994 Light and photosynthesis in aquatic ecosystems. Cambridge University Press.
- Larcombe P., Ridd P., Prytz A., Wilson B., 1995 Factors controlling suspended sediment on inner-shelf coral reefs, Townsville, Australia. *Coral reefs* 14:163-171.
- Likumahua S., 2013 Recent blooming of *Pyrodinium bahamense* var. *compressum* in Ambon Bay, Eastern Indonesia. *Marine Research in Indonesia* 38(1):31-37.
- Likumahua S., de Boer M. K., Krock B., Nieuwenhuizen T., Tatipatta W. M., Hehakaya S., Imu L., Abdul M. S., Moniharapon E., Buma A. G. J., 2019 First record of the dynamics of domoic acid producing Pseudo-nitzschia spp. in Indonesian waters as a function of environmental variability. *Harmful Algae* 90:101708.
- Loder T. C., Reichard R. P., 1981 The dynamics of conservative mixing in estuaries. *Estuaries* 4:64-69.
- Lu X., Mo Z., Zhao J., Ma C., 2024 Remote monitoring of water clarity in coastal oceans of the Guangdong-Hong Kong-Macao Greater Bay Area, China based on machine learning. *Ecological Indicators* 160:111789.
- Lugo-Fernández A., Gravois M., Montgomery T., 2008 Analysis of Secchi depths and light attenuation coefficients in the Louisiana-Texas shelf, northern Gulf of Mexico. *Gulf of Mexico Science* 26(1):2.
- Lunt J., Smee D. L., 2014 Turbidity influences trophic interactions in estuaries. *Limnology and Oceanography* 59(6):2002-2012.
- Macdonald R. K., 2015 Turbidity and light attenuation in coastal waters of the Great Barrier Reef. James Cook University, 232 pp.
- Male Y. T., Reichelt-Brushett A. J., Pocock M., Nanlohy A., 2013 Recent mercury contamination from artisanal gold mining on Buru Island, Indonesia–Potential future risks to environmental health and food safety. *Marine pollution bulletin* 77(1-2):428-433.
- Malone T. C., 1976 Phytoplankton production in the apex of the New York Bight, in: Gross, M.G. (Ed.), *The middle Atlantic Shelf and New York Bight*. Pp. 260-272.
- Matthes L., Ehn J., L.-Girard S., Pogorzelec N., Babin M., Mundy C., 2019 Average cosine coefficient and spectral distribution of the light field under sea ice: Implications for primary production. *Elem Sci Anth* 7:25.
- Mulhearn P., 1993 Distribution of turbidity in Australian Tropical Waters. Department of Defence, DSTO Materials Research Laboratory, 29 pp.

- Nurminen L., Horppila J., 2006 Efficiency of fish feeding on plant-attached prey: Effects of inorganic turbidity and plant-mediated changes in the light environment. *Limnology and Oceanography* 51(3):1550-1555.
- Ohlmann J. C., Siegel D. A., 2000 Ocean radiant heating. Part II: Parameterizing solar radiation transmission through the upper ocean. *Journal of Physical Oceanography* 30(8):1849-1865.
- Orpin A. R., Ridd P. V., 2012 Exposure of inshore corals to suspended sediments due to wave-resuspension and river plumes in the central Great Barrier Reef: A reappraisal. *Continental Shelf Research* 47:55-67.
- Pelasula D., 2008 [Impact of deforestation on upper land to marine coastal ecosystem on Ambon Bay], Faculty of Fishery and Marine Sciences. Universitas Pattimura, Ambon. Pp. 103. [in Indonesian]
- Pello F. S., Adiwilaga E. M., Huliselan N. V., Damar A., 2014 [Effect of seasonal on nutrient load input the inner Ambon Bay]. *Bumi Lestari Journal of Environment* 14(1):63-73. [in Indonesian]
- Pennock J. R., 1985 Chlorophyll distributions in the Delaware estuary: regulation by light-limitation. *Estuarine, Coastal and Shelf Science* 21(5):711-725.
- Pickard G., 1961 Oceanographic features of inlets in the British Columbia mainland coast. *Journal of the Fisheries Board of Canada* 18(6):907-999.
- Pownall J., Hall R., Watkinson I. M., 2013 Extreme extension across Seram and Ambon, eastern Indonesia: evidence for Banda slab rollback. *Solid Earth* 4(2):277-314
- Prasetyo B. A., Muawanah M., Mardianto L., Lubis M. Z., 2022 Spatial distributions of water quality parameters and their relationship to aquaculture activities in Lampung Bay. *Journal of Science and Applicative Technology* 6(1):1-11.
- Preisendorfer R. W., 1986 Secchi disk science: Visual optics of natural waters *Limnology and oceanography* 31(5):909-926.
- Reustle J. W., Smeed D. L., 2020 Cloudy with a chance of mesopredator release: Turbidity alleviates top-down control on intermediate predators through sensory disruption. *Limnology and Oceanography* 65(10):2278-2290.
- Riyadi A., 2005 Studies on water quality in coastal waters of Semarang City and the related suitability for aquaculture activities. *Jurnal Teknologi Lingkungan* 6(3):497-501.
- Saiya H. G., Dibyosaputro S., Santosa S. H. B., 2016 USLE estimation for potential erosion at Wae Heru Watershed and Wae Tonahitu Watershed, Ambon Island, Indonesia. *Indonesian Journal of Geography* 48(2):191-205.
- Salamena G. G., 2024 Secondary estuarine circulation and the related vertical mixing at the sill of Ambon Bay, eastern Indonesia. In *IOP Conference Series: Earth and Environmental Science*. 1329(1):012001.
- Salamena G. G., Heron S. F., Ridd P. V., Whinney J. C., 2023 A risk assessment of marine plastics in coastal waters of a small island: Lessons from Ambon Island, eastern Indonesia. *Regional Studies in Marine Science* 65c:103086.
- Salamena G. G., Whinney J. C., Heron S. F., 2022a Vertical circulation due to deep-water renewal and phytoplankton blooms in the tropical fjord of Ambon Bay, eastern Indonesia. *Journal of Marine Systems* 234:103776.
- Salamena G. G., Whinney J. C., Heron S. F., Ridd P. V., 2021 Internal tidal waves and deep-water renewal in a tropical fjord: lessons from Ambon Bay, eastern Indonesia. *Estuarine, Coastal and Shelf Science* 253:107291.
- Salamena G. G., Whinney J. C., Heron S. F., Ridd P. V., 2022b Frontogenesis and estuarine circulation at the shallow sill of a tropical fjord: Insights from Ambon Bay, eastern Indonesia. *Regional Studies in Marine Science* 56:102996.
- Shen F., Verhoef W., Zhou Y., Salama M. S., Liu X., 2010 Satellite estimates of wide-range suspended sediment concentrations in Changjiang (Yangtze) estuary using MERIS data. *Estuaries and Coasts* 33:1420-1429.

- Shen F., Zhou Y., Li J., He Q., Verhoef W., 2013 Remotely sensed variability of the suspended sediment concentration and its response to decreased river discharge in the Yangtze estuary and adjacent coast. *Continental Shelf Research* 69:52-61.
- Sidabutar T., Praseno D. P., Fukuyo Y., 2000 Harmful algal blooms in Indonesian waters, the Ninth International Conference on Harmful Algal Blooms Hobart, Australia. Pp. 124-128.
- Sidabutar T., Srimariana E. S., Cappenberg H. A. W., Wouthuyzen S., 2022 Harmful algal bloom of the three selected coastal bays in Indonesia. In IOP Conference Series: Earth and Environmental Science. 1119(1):012035.
- Siregar V., Koropitan A. F., 2013 Primary productivity of Jakarta Bay in a changing environment: anthropogenic and climate change impacts. *Biotropia* 20(2):89-103.
- Smith L. M., Engle V. D., Summers J. K., 2006 Assessing water clarity as a component of water quality in Gulf of Mexico estuaries. *Environmental monitoring and assessment* 115(1):291-305.
- Sokoletsky L., Shen F., 2013 Turbidity classification of Chinese natural waters, Asian Workshop on Ocean Color (AWOC). Pp. 3-5.
- Syahailatua A., Wouthuyzen S., Pelasula D. D., 2012. Coral reefs in ambon bay need sustainable management: Insights from 40 years of monitoring. *RIN Dataverse*.
- Syvitski J. P., Burrell D. C., Skei J. M., 2012 Fjords: processes and products. Springer Science & Business Media. Pp. 277-278.
- Tarigan M. S., 1989 [Air and sea surface temperatures of the outer Ambon Bay]. Pusat Penelitian dan Pengembangan Oseanologi LIPI, Ambon. Pp. 35. [in Indonesian]
- Turner J. S., Friedrichs C. T., Friedrichs M. A., 2021 Long-Term Trends in Chesapeake Bay Remote Sensing Reflectance: Implications for Water Clarity. *Journal of Geophysical Research: Oceans* 126(12):e2021JC017959.
- Tyler J. E., 1968 The secchi disc. *Limnology and oceanography* 13(1):1-6.
- Uncles R., Stephens J., Smith R., 2002 The dependence of estuarine turbidity on tidal intrusion length, tidal range and residence time. *Continental shelf research* 22(11-13):1835-1856.
- Van Oostenbrugge J. A. E., 2003 Uncertainty in daily catch rate in the light fisheries around Ambon and the Lease Islands: characterisation, causes and consequences. Wageningen University, Wageningen, The Netherlands, 200 pp.
- Vantrepotte V., Loisel H., Dessailly D., Mériaux X., 2012 Optical classification of contrasted coastal waters. *Remote Sensing of Environment* 123:306-323.
- Vogel J. L., Beauchamp D. A., 1999 Effects of light, prey size, and turbidity on reaction distances of lake trout (*Salvelinus namaycush*) to salmonid prey. *Canadian Journal of Fisheries and Aquatic Sciences* 56(7):1293-1297.
- Wei J., Lee Z., 2013 Model of the attenuation coefficient of daily photosynthetically available radiation in the upper ocean. *Methods in Oceanography* 8:56-74.
- Weiskerger C. J., Rowe M. D., Stow C. A., Stuart D., Johengen T., 2018 Application of the Beer-Lambert model to attenuation of photosynthetically active radiation in a shallow, eutrophic lake. *Water Resources Research* 54(11):8952-8962.
- Wenno L. F., 1989 [Notes on the optical properties of Ambon Bay]. Pusat Penelitian dan Pengembangan Oseanologi LIPI, Ambon, 28 pp. [in Indonesian]
- Wenno L. F., Anderson J. J., 1984 Evidence for tidal upwelling across the sill of Ambon Bay. *Marine Research in Indonesia* 23:13-20.
- Whinney J., Jones R., Duckworth A., Ridd P., 2017 Continuous in situ monitoring of sediment deposition in shallow benthic environments. *Coral Reefs* 36(2):521-533.
- Wofsy S. C., 1983 A simple model to predict extinction coefficients and phytoplankton biomass in eutrophic waters *Limnology and Oceanography* 28(6):1144-1155.
- Workgroup F. S. S. R., 2004 Factors influencing seagrass recovery in Feather Sound, Tampa Bay, Florida.

Received: 11 December 2024. Accepted: 21 March 2025. Published online: 21 March 2025.

Authors:

Richard R. Lokollo, Marine Sciences Study Program, Postgraduate Program of Pattimura University, Jl. Ir. M. Putuhena, 97233 - Ambon, Indonesia; Department of Physics, Faculty of Sciences and Technology, Pattimura University, Jl. Ir. M. Putuhena, 97233 - Ambon, Indonesia, e-mail: richard.lokollo@lecturer.unpatti.ac.id
Alex S. W. Retraubun, Department of Marine Sciences, Faculty of Fisheries and Marine Sciences, Pattimura University, Jl. Mr. Chr. Soplanit, 97233 - Ambon, Indonesia, e-mail: alex.retraubun@lecturer.unpatti.ac.id
Simon Tubalawony, Department of Marine Sciences, Faculty of Fisheries and Marine Sciences, Pattimura University, Jl. Mr. Chr. Soplanit, 97233 - Ambon, Indonesia, e-mail: simon.tubalawony@lecturer.unpatti.ac.id
Harold J. D. Waas, Department of Marine Sciences, Faculty of Fisheries and Marine Sciences, Pattimura University, Jl. Mr. Chr. Soplanit, 97233 - Ambon, Indonesia, e-mail: harold.waas@lecturer.unpatti.ac.id
Sem Likumahua, Research Center for Deep Sea, National Research and Innovation Agency (BRIN), Jl. Pasir Putih I, Ancol Timur, 14430 - Jakarta, Indonesia; Center for Collaborative Research on Aquatic Ecosystems in Eastern Indonesia, Jl. Dr. J. Leimena, 97233 - Ambon, Indonesia, e-mail: sem.likumahua@brin.go.id
Gerry G. Salamena, Research Center for Deep Sea, National Research and Innovation Agency (BRIN), Jl. Pasir Putih I, Ancol Timur, 14430 - Jakarta, Indonesia; Center for Collaborative Research on Aquatic Ecosystems in Eastern Indonesia, Jl. Dr. J. Leimena, 97233 - Ambon, Indonesia, e-mail: gerry.gilliant.salamena@brin.go.id
This is an open-access article distributed under the terms of the Creative Commons Attribution License, which permits unrestricted use, distribution, and reproduction in any medium, provided the original author and source are credited.

How to cite this article:

Lokollo R. R., Retraubun A. S. W., Tubalawony S., Waas H. J. D., Likumahua S., Salamena G. G., 2025 Water clarity characteristics during rainfall season revealing impacts of deforestation on the fjord-like basin of inner Ambon Bay in the small island of Ambon, eastern Indonesia. *AAFL Bioflux* 18(2):658-678.